Electronic Supplementary Material (ESI) for RSC Advances.
This journal is © The Royal Society of Chemistry 2018

Supporting Information

to the manuscript

Effect of additives, ball milling and isotopic exchange in porous magnesium borohydride

Michael Heere[a,b,*], Olena Zavorotynska[a,c], Stefano Deledda[a], Magnus H. Sørby[a], David Book[d], Theodore Steriotis[e] and Bjørn C. Hauback[a]

[a] Department for Neutron Materials Characterization, Institute for Energy Technology, NO–2027 Kjeller, Norway

[b] Institute for Applied Materials – Energy Storage Systems (IAM-ESS), Karlsruhe Institute of Technology (KIT), D–76344, Eggenstein–Leopoldshafen, Germany

[c] Institute for Mathematics and Physics, University of Stavanger, P.O.Box 8600 Forus, NO-4036 Stavanger, Norway

[d] School of Metallurgy and Materials, University of Birmingham, Birmingham B15 2TT, United Kingdom

[e] Institute of Nanoscience and Nanotechnology, NCSR “Demokritos”, Ag. Paraskevi Attikis, Athens 15341, Greece

Keywords: gas-solid exchange, hydrogen isotopic exchange, magnesium borohydride, *in situ* Raman spectroscopy, hydrogen storage, specific surface area

PART A

Fig. A1

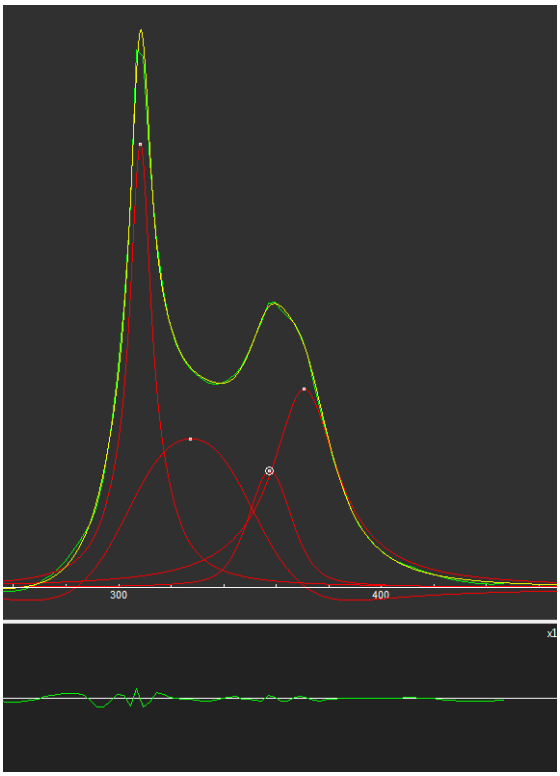

Fig. A1 DSC data of γ-$Mg(BH_4)_2$+Ni_3B heated from RT - 450 °C at 7 °C min^{-1}. The peak fitting function in Fityk (M. Wojdyr, Appl. Cryst. (2010). 43, 1126-1128) is used for determination of the peak position (peak temperatures). The right part is baseline corrected with the red curves showing the four decomposition steps in γ-$Mg(BH_4)_2$, which results as summation into the yellow curve. The original data is shown in the green curve. The green curve at the bottom shows the difference plot.

Fig. A2

TG data were employed to calculate the deuterium content. For this, the TG data for the four measurements were averaged. The value which differed most from the average was excluded as an outlier. This procedure was necessary as the TG data determination includes a baseline correction, which was found to deviate strongly for the heating rate of 2 °C min^{-1}. All data including and excluding the outlier and respective standard deviations are given in Fig. A2. The TG data of samples treated in 3 bar D_2 is based on the average of three measurements including the standard deviation. The deuterium content "x" in $Mg(BH_{4-x}D_x)_2$ was calculated from the TG data under the assumption that the measured mass losses are due to complete H+D desorption from the materials." A constant isotopic exchange was assumed.

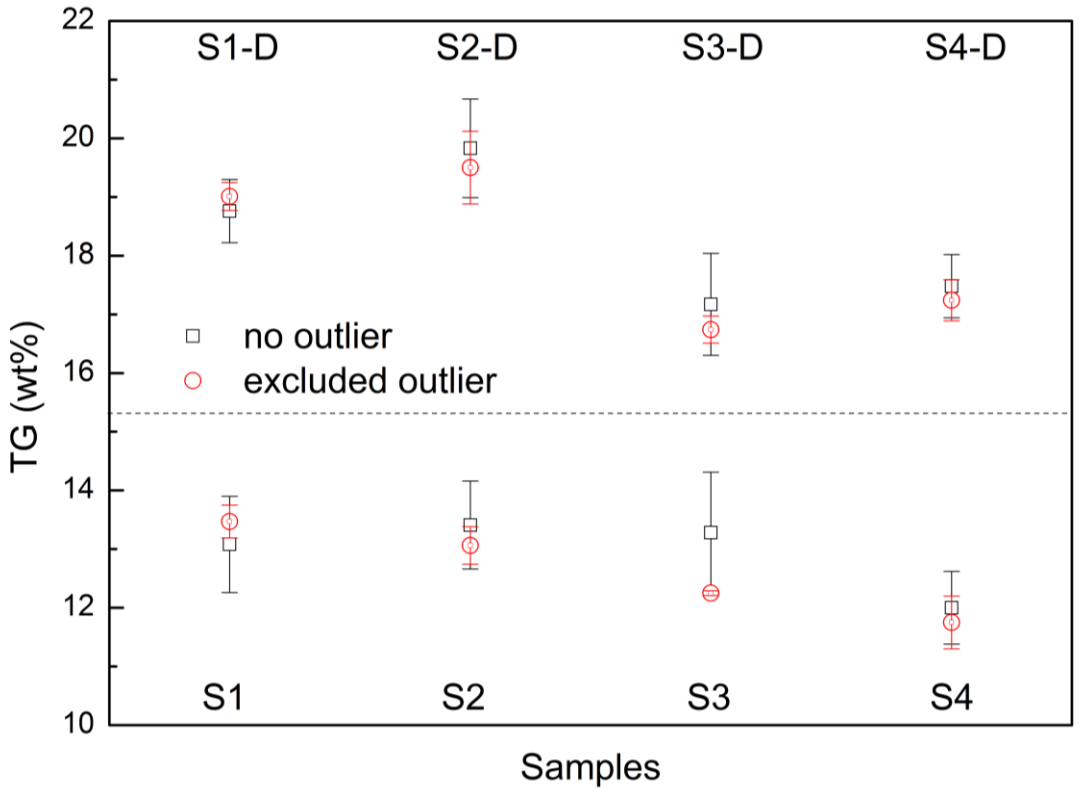

Fig. A2a TG data including the standard deviation of pure samples S1-S4 (down) and H→D exchanged samples, S1-D to S4-D (up). Black data points with no outlier (4 measurements), red data points with exclusion of one outlier.

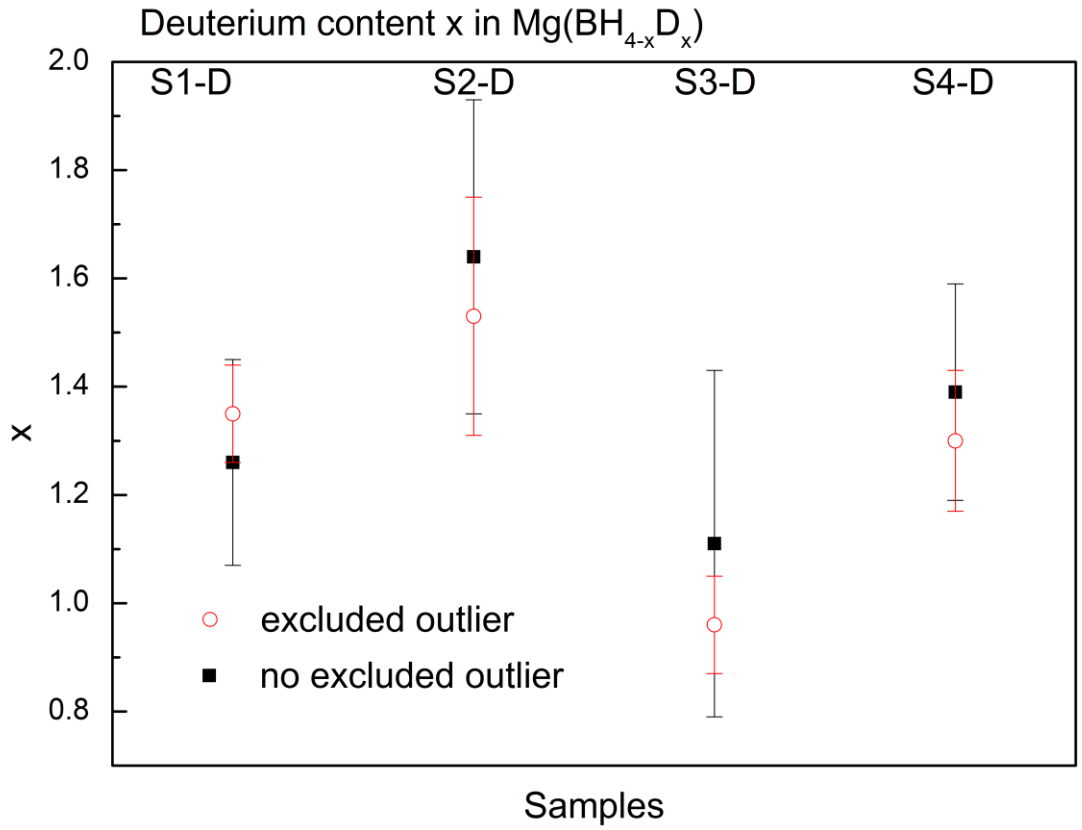

Fig. A2b Deuterium content including the standard deviation calculated from TG data of H→D exchanged samples, S1-D to S4-D. Black data points with no outliers (4 measurements), red data points with exclusion of one outlier.

Figures A3

Decomposition step I is the first decomposition event connected with the release of hydrogen and with the formation of amorphous Mg-B-H phases. Step II could be assigned to the formation of MgH_2, which is an exothermic process. Step III is the decomposition of the amorphous Mg-B-H phases which subsequently form amorphous boron and step IV can be assigned to the decomposition of the newly formed MgH_2.

Fig. A3a - S1

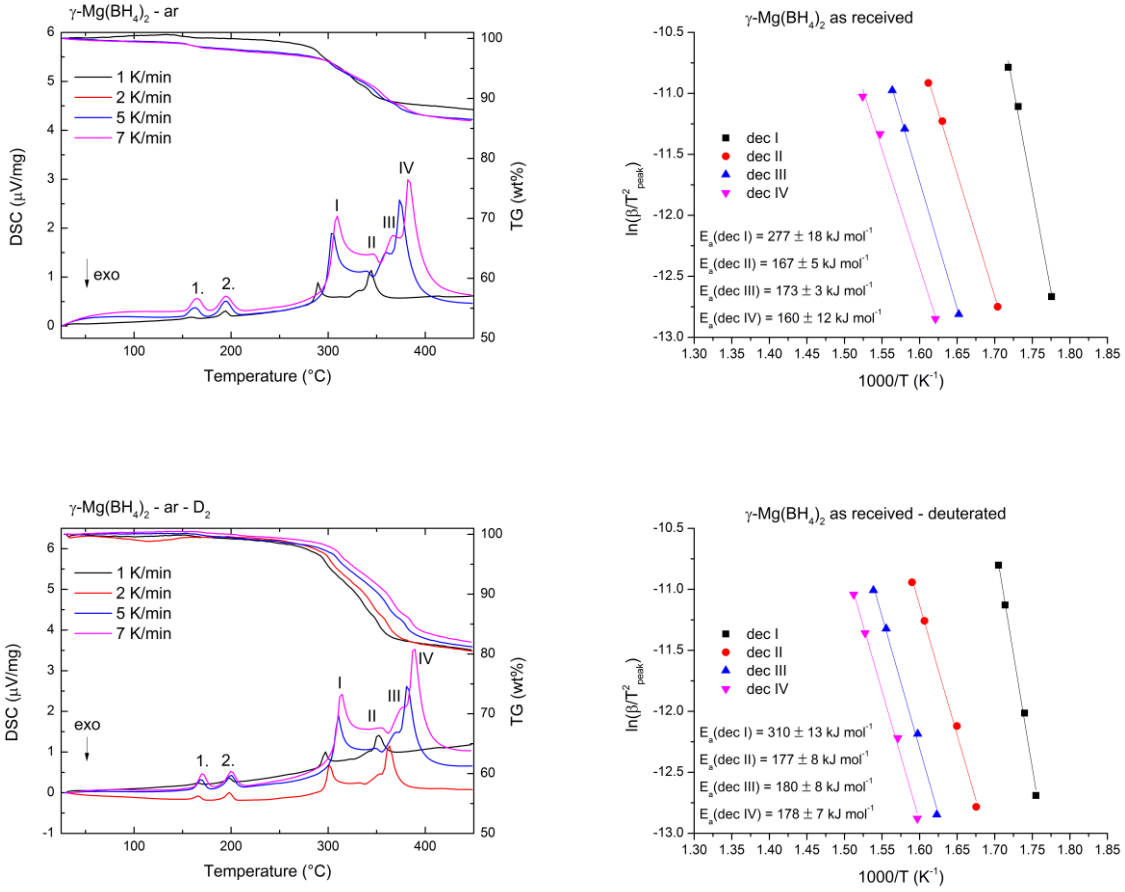

Fig. A3a TG-DSC measurements (left) of as received (ar) γ-$Mg(BH_4)_2$ (top) and H→D exchanged γ-$Mg(BH_4)_2$ (bottom) with the activation energies from the measurements shown on the right. 1. and 2. mark the phase transition, while the steps of decomposition (dec) are shown.

Fig. A3b - S2

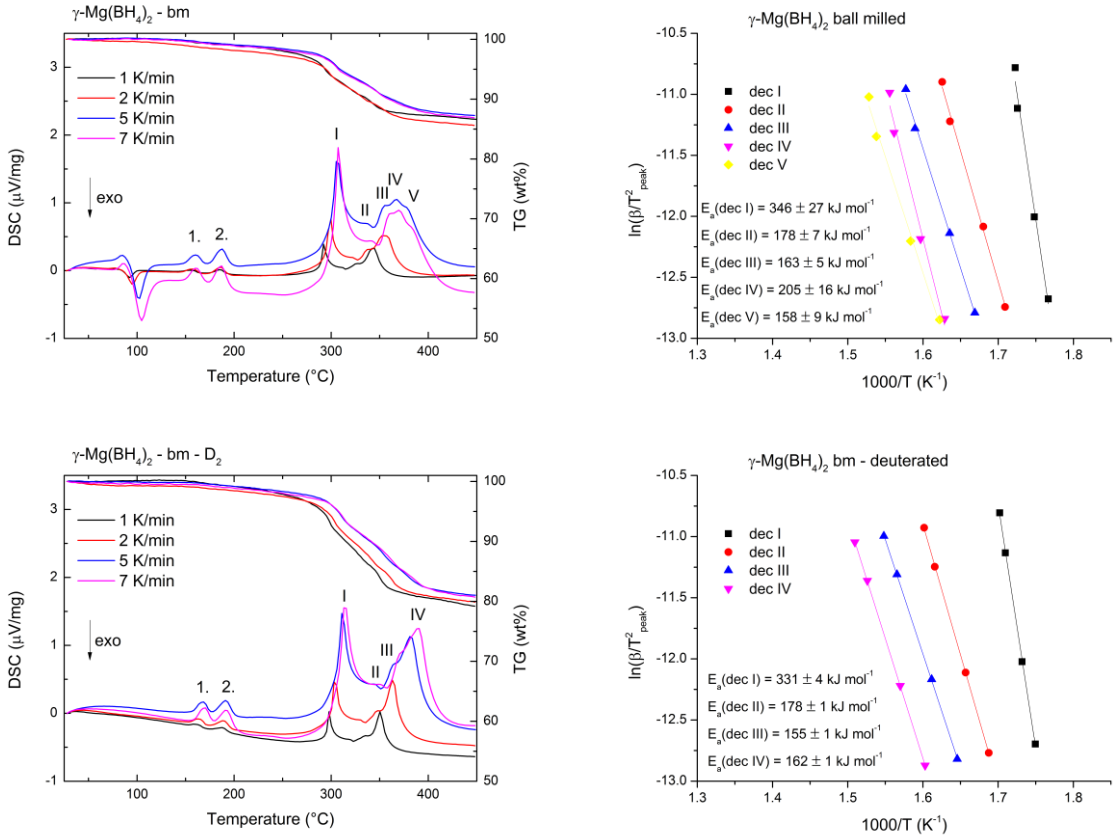

Fig. A3b TG-DSC measurements (left) of ball milled (bm) γ-$Mg(BH_4)_2$ (top) and H→D exchanged γ-$Mg(BH_4)_2$ (bottom) with the activation energies from the measurements shown on the right. 1. and 2. mark the phase transition, and the steps of decomposition (dec) are shown.

Fig. A3c - S3

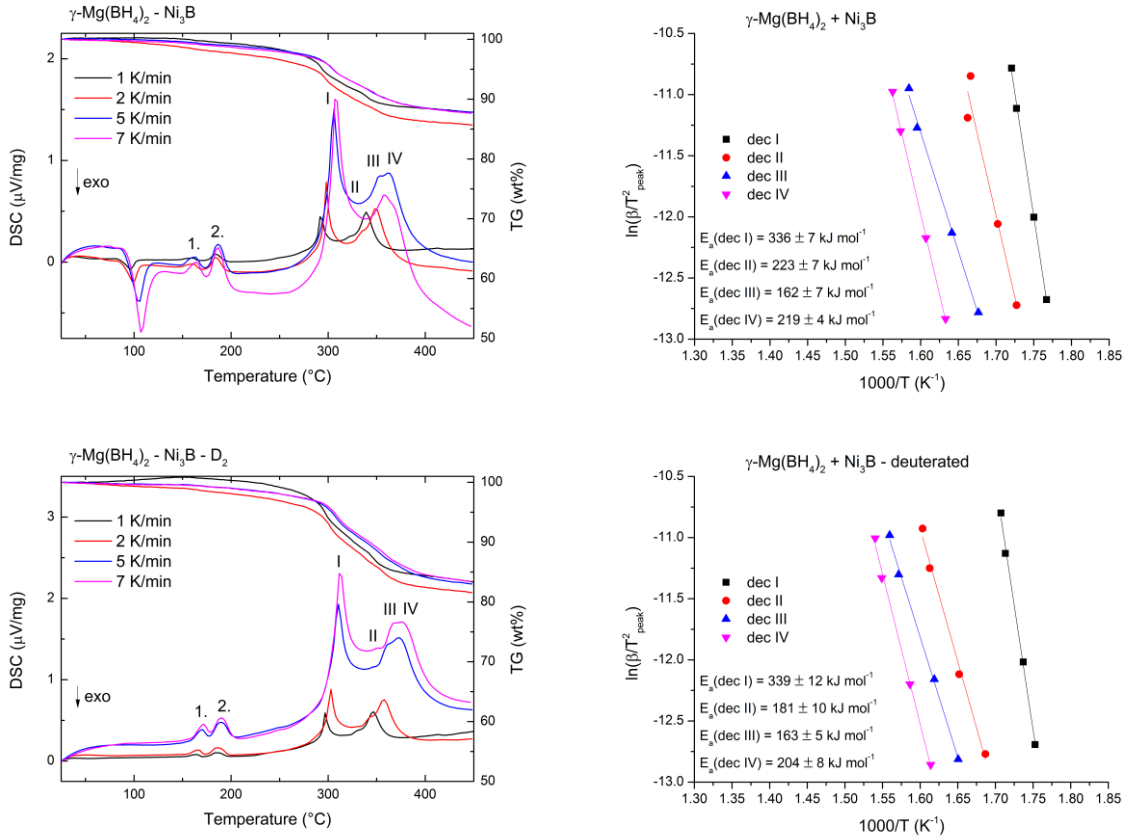

Fig. A3c TG-DSC measurements (left) of γ-$Mg(BH_4)_2$ + Ni_3B (top) and H→D exchanged γ-$Mg(BH_4)_2$ + Ni_3B (bottom) with the activation energies from the measurements shown on the right. 1. and 2. mark the phase transition, and the steps of decomposition (dec) are shown.

Fig. A3d - S4

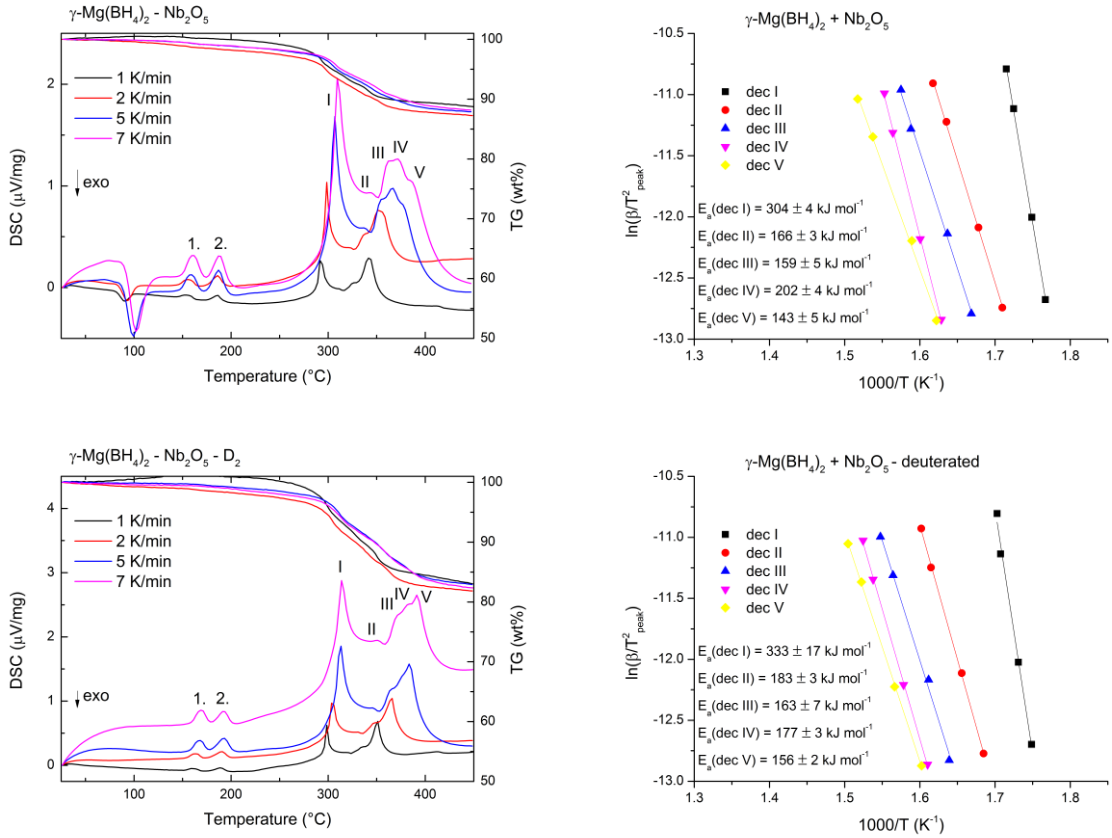

Fig. A3d TG-DSC measurements (left) of γ-$Mg(BH_4)_2$ + Nb_2O_5 (top) and H→D exchanged d γ-$Mg(BH_4)_2$ + Nb_2O_5 (bottom) with the activation energies from the measurements shown on the right. 1. and 2. mark the phase transition, and the steps of decomposition (dec) are shown.

Fig. A4

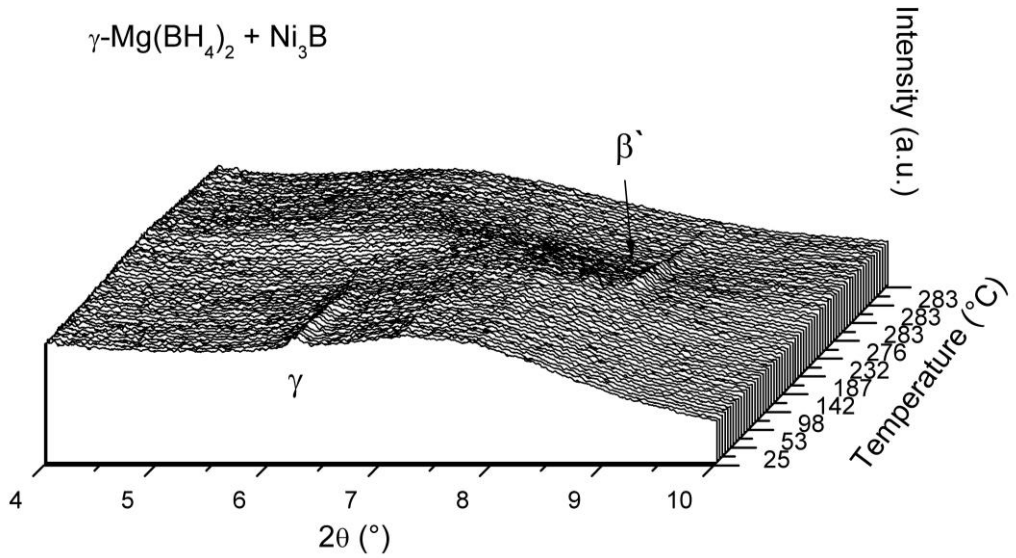

Fig. A4 *In situ* SR-PXD data of ball milled $Mg(BH_4)_2$ + Ni_3B heated from RT to 285 °C under 2 bar H_2 (temperature ramp of 5 °C min^{-1}) and 0.5 h isotherm. λ = 0.6973 Å. Bragg peaks from γ- and β'-$Mg(BH_4)_2$ are indicated.

Fig. A5

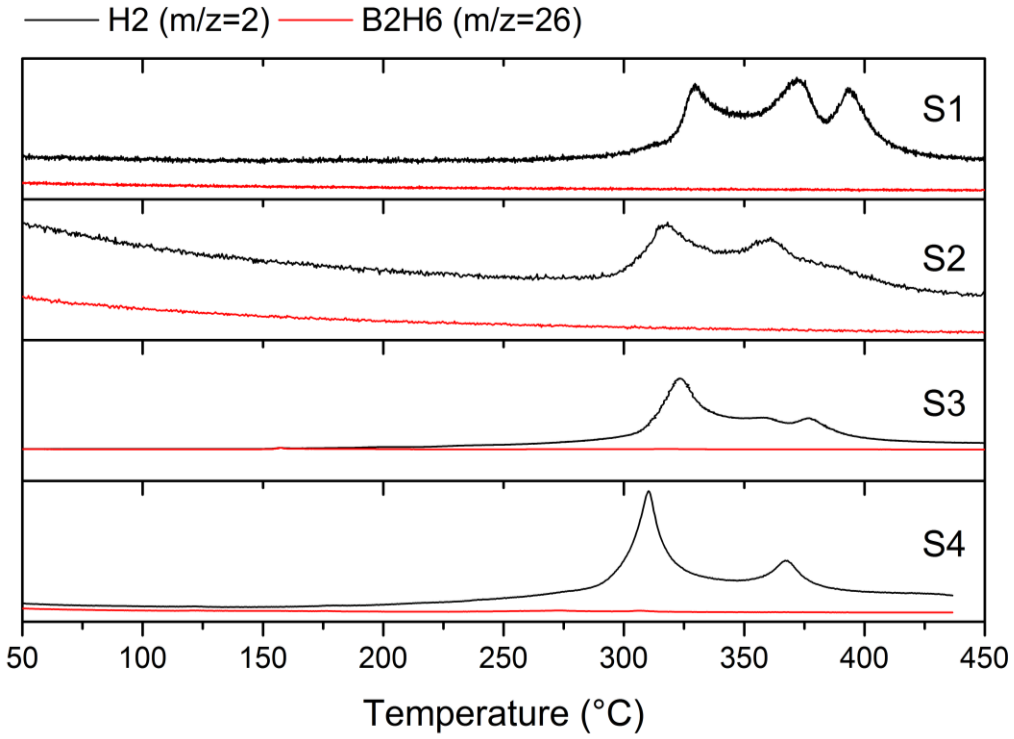

Fig. A5 TPD-MS data of S1-S4 during heating from RT - 450 °C showing the release of H_2 (black curves), B_2H_6 (red curves).

Fig. A6

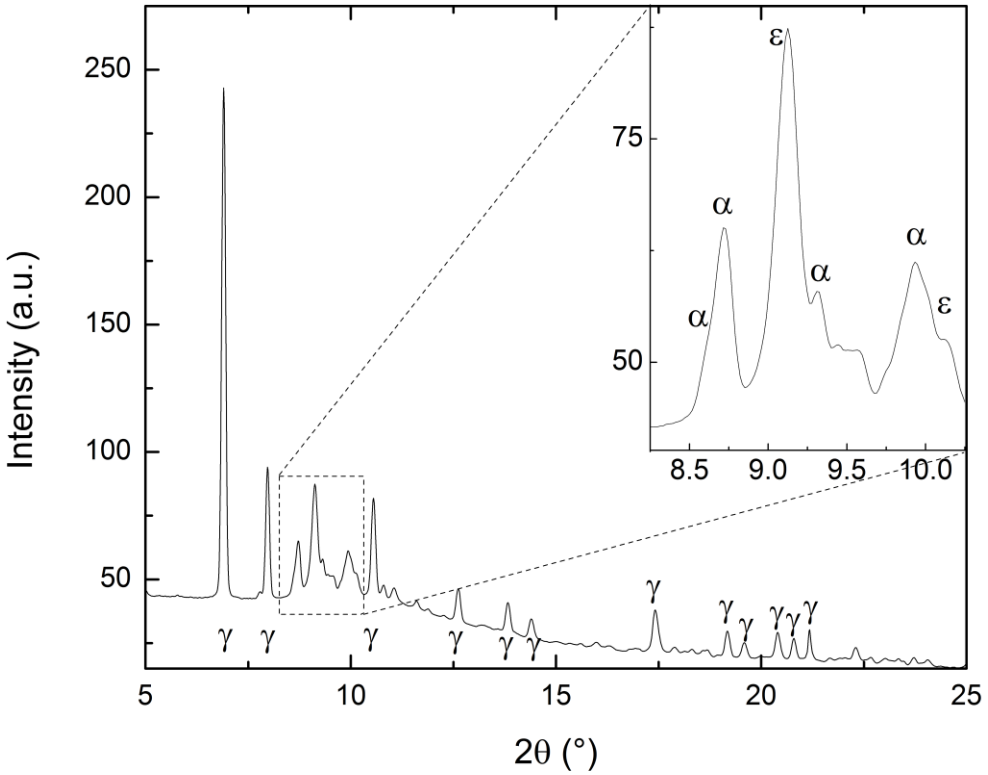

Fig. A6 SR-PXD data of H→D exchanged $Mg(BH_4)_2$ after heat treatment and cooling to RT. The heat treatment proceeded from RT to 180 °C under 1 bar argon in boron glass capillary with a heating ramp of 5 °C min^{-1} to 162 °C followed by an isotherm for 35 min, at 175 °C for 9 min and finally 180 °C for 53 min. The SR-PXD data, collected 16 hours after reaching RT, show a mixture of γ-, α-, and ε-$Mg(BH_4)_2$. Inset shows magnification of ε-$Mg(BH_4)_2$ phase at RT. λ = 0.7753 Å.

A control experiment was conducted, to see if ε–$Mg(BH_4)_2$ is also stable at RT for S1–D. In Fig. A6 the SR–PXD data show Bragg peaks of ε–$Mg(BH_4)_2$ at RT after heating S1–D to 180 °C and a 16 h waiting period at RT. This observation confirms that the phase transition temperature was not reached during exposure to a deuterium atmosphere, thus, explaining the lack of Bragg peaks from ε–$Mg(BH_4)_2$ in S1–D.

Fig. A7

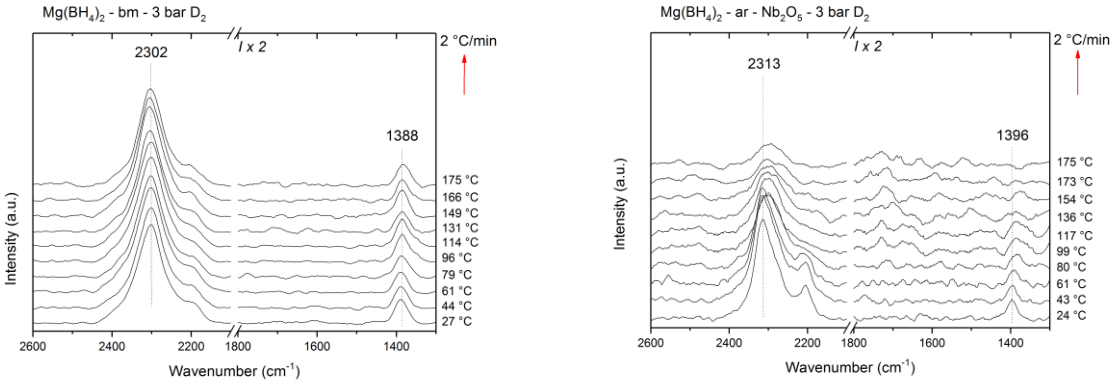

Fig. A7 *In situ* Raman with heating from RT to 175 °C at 2 K min^{-1}. Every 10^{th} measurement is shown. Left: ball milled $Mg(BH_4)_2$ (S2) under 3 bar D_2; right: as received $Mg(BH_4)_2$ + 3 mol% Nb_2O_5 (S5) under 3 bar D_2; all data is translated in y axis for better visualization.

Table A1 - Activation energies

Table A1 Activation energies for up to 5 different steps of decomposition with straight line fitting error.

Name/decomposition step	#	E_a (dec I)	E_a (dec II)	E_a (dec III)	E_a (dec IV)	E_a (dec V)	Ref
as received $Mg(BH_4)_2$	S1	275 ± 10	167 ± 5	173 ± 3	160 ± 12		this work
as received $Mg(BH_4)_2$		244 ± 17	157 ± 7	156 ± 7	139 ± 12		[1]
as received $Mg(BH_4)_2$ - D_2	S1-D	310 ± 13	177 ± 8	180 ± 8	178 ± 7		this work
ball milled $Mg(BH_4)_2$	S2	346 ± 27	178 ± 8	163 ± 5	205 ± 16	158 ± 9	this work
ball milled $Mg(BH_4)_2$ - D_2	S2-D	331 ± 4	178 ± 1	155 ± 1	162 ± 1		this work
$Mg(BH_4)_2$ + Ni_3B	S3	336 ± 7		162 ± 7	219 ± 4		this work
$Mg(BH_4)_2$ + Ni_3B - D_2	S3-D	339 ± 12	181 ± 10	163 ± 5	204 ± 8		this work
$Mg(BH_4)_2$ + Nb_2O_5	S4	304 ± 4	166 ± 3	159 ± 5	202 ± 4	143 ± 5	this work
$Mg(BH_4)_2$ + Nb_2O_5 - D_2	S4-D	333 ± 17	183 ± 3	163 ± 7	177 ± 3	156 ± 2	this work

Table A2 Area (A) of B–H stretching region [A ν_{B-H}] (2500–1900 cm^{-1}) before H→D exchange and [A ν_{B-H}]' (2500–2000 cm^{-1}) after 23 h in 3 bar D_2. Area of B–D stretching region ν_{B-D} (1900–1500 cm^{-1}), noted as [A ν_{B-D}]' after 23 h in 3 bar D_2.

	S1	S2	S3	S4
[Aν_{B-H}]	208 ± 4	268 ± 2	279 ± 4	270 ± 2
	S1–D	S2–D	S3–D	S4–D
[Aν_{B-H}]'	174 ± 1	175 ± 3	195 ± 5	176 ± 12
[Aν_{B-D}]'	420 ± 3	415 ± 2	254 ± 1	355 ± 4

PART B – Adsorption measurements

Adsorption isotherms were carried out on an Autosorb-1MP volumetric analyzer equipped with a Gifford-McMahon cryocooler. Preliminary N_2 adsorption measurements of the as received sample at 77 K revealed extremely poor kinetics. For this reason very strict equilibration criteria were employed, while due to the ultra-microporous character of the sample low relative pressure measurements were selected, both leading to very time consuming measurements. It should further be noted that helium was used for volume calibrations at room and liquid nitrogen temperature under the assumptions that (a) helium is not sorbed on the samples and (b) helium does not penetrate into regions which are inaccessible for nitrogen. The above are not necessarily true for ultra-microporous materials and for this reason the results obtained may underestimate the amounts adsorbed (and thus BET areas, pore volumes, etc). For the case of S1 approximately 20 mg of material were used. The sample was outgassed at 35 °C under vacuum for 10 h. Fig. B1 shows the full N_2 adsorption/desorption isotherm (16000 min measuring time) of the as received γ-$Mg(BH_4)_2$ sample (inset shows semilog scale). The isotherm is type I, according to the IUPAC classification, with no hysteresis, revealing a purely microporous character.

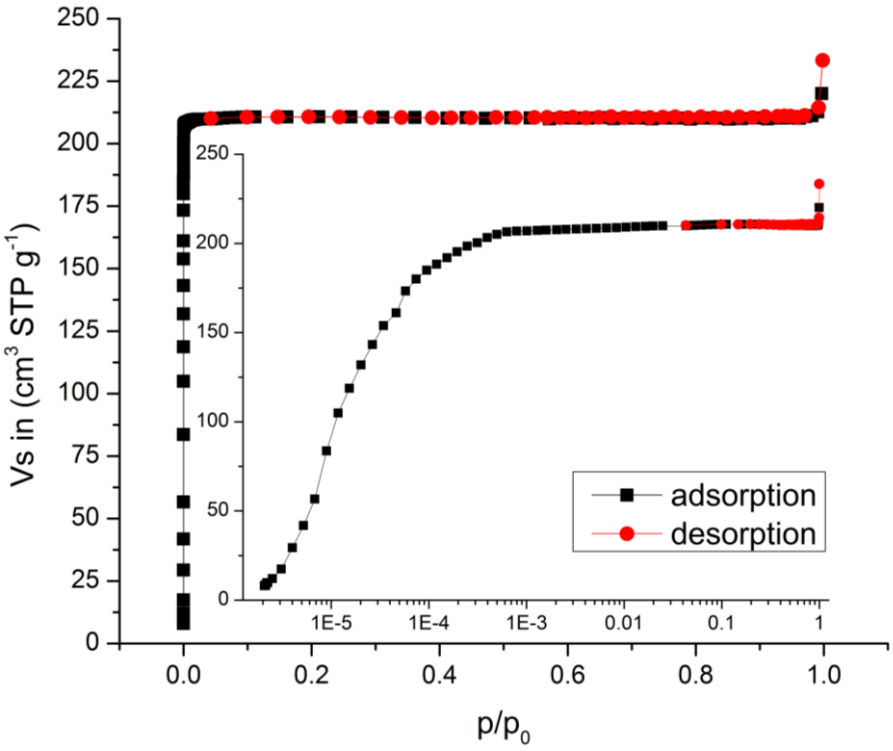

Fig. B1 N_2 adsorption-desorption isotherm (77 K) of the as received γ-$Mg(BH_4)_2$.

The N_2 isotherm was further analyzed in terms of pore volume and surface area. The pore volume (0.327 cm^3/g) was calculated from the amount sorbed at p/p_0=0.98 by assuming that the adsorbed phase has the density of liquid N_2 (0.808 g/cm^3). For an estimation of the specific surface area of the sample several methods were used and the pertinent results are summarized in Table 3.

On the contrary, the ball milled sampled (S2) revealed very limited adsorption capacity. The N_2 adsorption-desorption isotherm (Fig. B2) is practically type II (IUPAC), which is typical for non-porous solids and as such no pore volume can be calculated. The miniscule hysteresis observed is attributed to a small amount of inter-particle porosity. The surface area data are reported in Table 3.

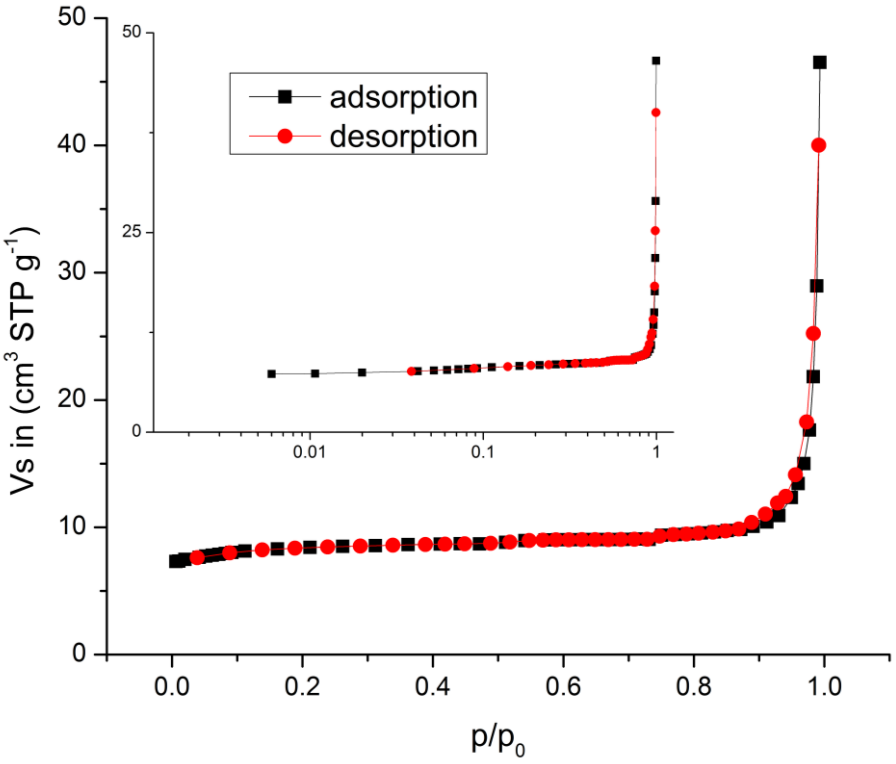

Fig. B2 N_2 adsorption-desorption isotherm (77 K) of the ball milled γ-$Mg(BH_4)_2$.

The ball milled sample (S2) was further thermally treated for 23 hours, at 120 °C, under hydrogen back pressure of 3 bar to exclude any possible $Mg(BH_4)_2$ decomposition, and renamed to S2-H. Following this treatment ~11 mg of the ball-milled-thermally treated sample was transferred to an Autosorb cryocooler cell and the N_2 adsorption-desorption isotherm was measured at 77 K. Identical equilibration criteria with the case of S1 were used (however starting from a slightly higher relative pressure, i.e. $6x10^{-6}$) and the experiment lasted for around 5500 min. The data are presented in Fig. B3. It can be seen directly from the sorption isotherms (Fig. B1 and B3) that the γ-$Mg(BH_4)_2$ structure was re-established, however, only partially since the total pore volume calculated for the thermally treated sample is 0.204 cm^3/g. Therefore, only ~62% of the pore volume of the as received γ-

$Mg(BH_4)_2$ is accessible to N_2 at 77 K. Likewise, the calculated surface areas (Table 6) are lower (by ~38%) compared to S1.

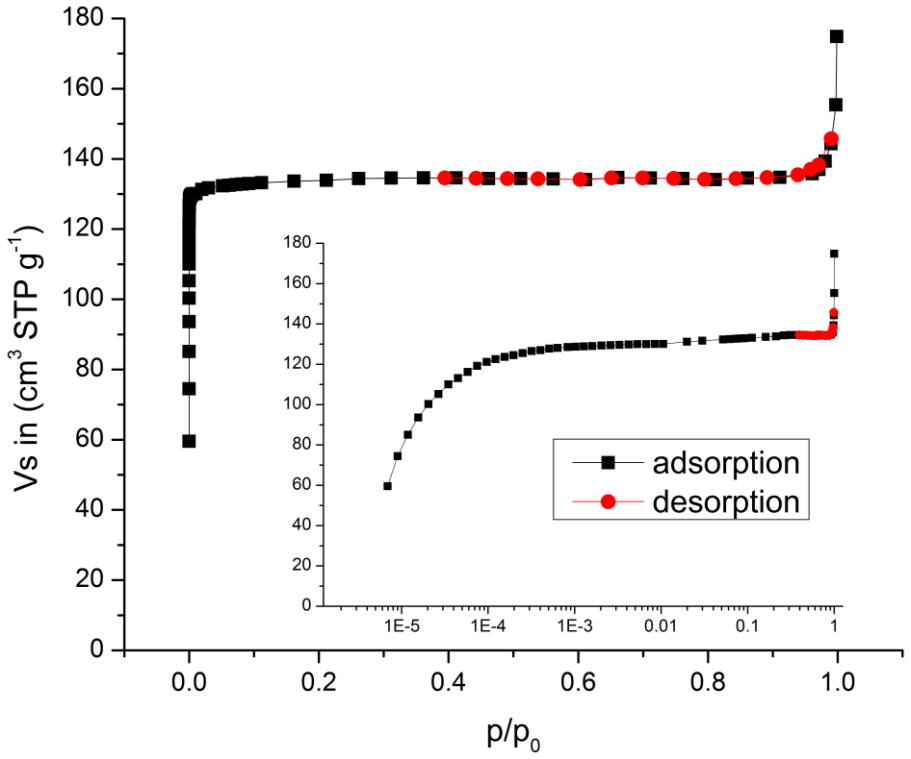

Fig. B3 N_2 adsorption-desorption isotherm (77 K) of the ball milled and thermally treated γ-$Mg(BH_4)_2$.

For comparison the as received sample (S1) was also thermally treated for 23 hours, at 120 °C, under hydrogen back pressure of 3 bar (renamed to S1-H) and consequently similar N_2 adsorption-desorption measurements with S1 were carried out at 77 K on ~13 mg of material. The experiment lasted for appr. 5200 min and the data are presented in Fig. B4. It can be seen directly from the sorption isotherms (Fig. B1 and B4) that a part of the porous structure of γ-$Mg(BH4)_2$ structure was not accessible since the total pore volume calculated for the thermally treated sample is 0.250 cm^3/g, i.e. only ~76.5% of the pore volume of the as-received sample. Likewise the calculated surface areas (Table 6) are lower than the as-received sample (again the 76.5% of the initial area).

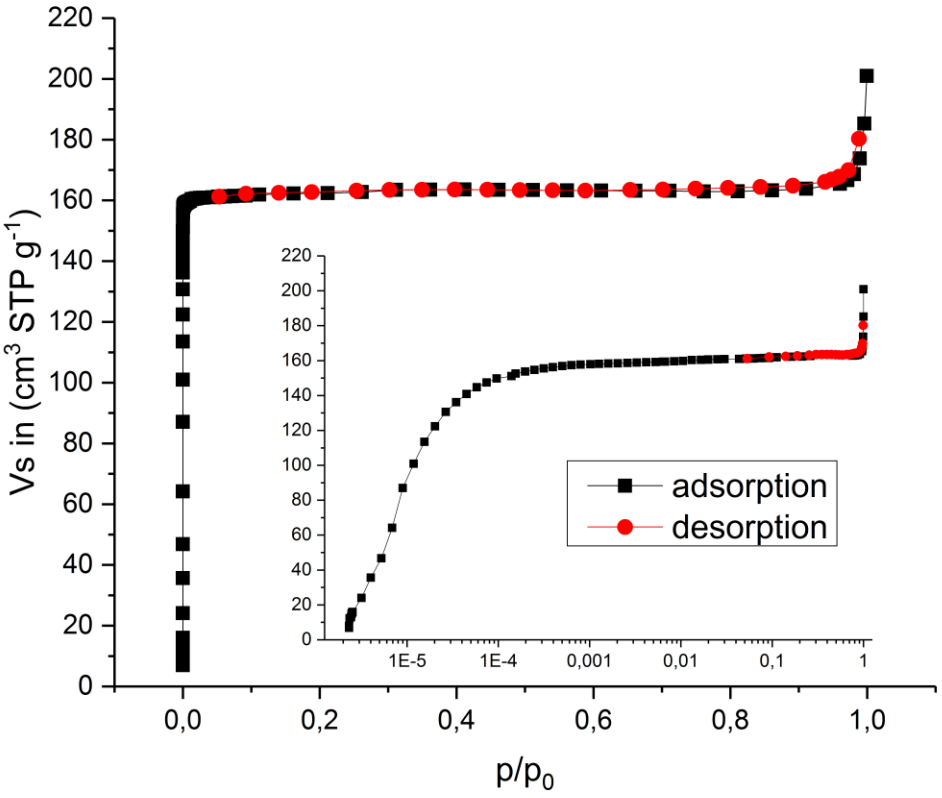

Fig. B4 N_2 adsorption-desorption isotherm (77 K) of the as-received thermally treated γ-$Mg(BH_4)_2$

It should be noted that a common feature of all the isotherms measured (apart from the non-porous S2 sample) was extremely low adsorption kinetics leading to significantly long equilibration times (more than a day/point for low vapor pressures). This situation is a typical sign of steric hindrance in severely constricted pore networks or partial pore blocking (by e.g. amorphous material), and in such case the accessibility of all the pore volume by the adsorbate molecules is doubtful within logical time-frames. In this respect the results should be treated with precaution. However the overall qualitative picture is valid beyond any doubt. S1 has a high surface area part of which becomes inaccessible after heat treatment (due to partial amorphization and/or constrictions). The ball milled S2 sample is 100% non-porous, however upon heat treatment the major part of the material recrystallizes and becomes highly porous (again part of the material remains amorphous and/or constrictions render part of the porous structure inaccessible to N_2 at 77K).

References

1 O. Zavorotynska, A. El-Kharbachi, S. Deledda and B. C. Hauback, *International Journal of Hydrogen Energy*, 2016, **41**, 14387.